Organic & Biomolecular Chemistry

RSC Publishing

PAPER

View Article Online
View Journal | View Issue

Cite this: *Org. Biomol. Chem.*, 2013, **11**, 746

Synthesis and structural studies of S-type/N-type-locked/frozen nucleoside analogues and their incorporation in RNA-selective, nuclease resistant 2′–5′ linked oligonucleotides†

Namrata Erande,[a] Anita D. Gunjal,[a] Moneesha Fernandes,[a] Rajesh Gonnade[b] and Vaijayanti A. Kumar*[a]

Received 4th May 2012,
Accepted 7th November 2012

DOI: 10.1039/c2ob26762d

www.rsc.org/obc

2′-*endo* locked or frozen (S-type)/3′-*endo* locked or frozen (N-type) nucleoside analogues were synthesized. Conformational analysis based on $^{3}J_{HH}$ and NOE measurements is presented which is further confirmed by X-ray crystal structural studies. 2′–5′ *iso*DNA oligonucleotides (ON) were synthesized using these modified nucleoside analogues and UV-T_m studies of the resultant 2′–5′ *iso*DNA : RNA duplexes reflect the site- and sequence-dependent effects and confirm that the S-type sugar conformations were preferred over the N-type sugar geometry in such duplexes.

Introduction

The antisense therapeutic approach discovered more than three decades ago by Zamecnik and Stephenson[1,2] continues to attract chemists towards the design and synthesis of modified antisense oligonucleotides (ASOs) till today, now with a renewed interest, especially with the potential applications in siRNA[3] and miRNA[4] therapeutic targeting.

Preorganization of the structure of an oligonucleotide single strand so as to match the structure of the duplex form, can lead to increased duplex stability due to entropic advantage. The concept of conformational restriction[5] has come to the forefront for application in nucleic acid chemistry as seen in a variety of analogues such as locked nucleic acids (LNA/BNA),[6] hexitol nucleic acid (HNA)[7] and tricyclic DNA (tcDNA),[8] all of which show increased affinity towards complementary RNA with very high fidelity and without compromising specific base-pairing properties. The 2′–5′ linked *iso*DNA/*iso*RNA are a unique class of oligonucleotides that bind exclusively only to RNA targets and not to their DNA counterparts.[9] This interesting aspect of 2′–5′ linked oligonucleotides has not been exploited for their applications in antisense research probably because of the relatively poor stability of the *iso*DNA/*iso*RNA : RNA duplexes. Damha *et al.* synthesized 2′–5′ RNA[9] (*iso*RNA) which occurs naturally[10] but does not encode genetic information. This synthesized *iso*RNA exhibited self-pairing as well as pairing with RNA,[9] but did not complex with complementary DNA. The CD patterns of *iso*RNA : RNA duplexes were found to be very similar to those of the natural 3′-5′DNA : RNA duplexes, indicating comparable overall structures *i.e.*, compact A-form duplex structure.[11] Solution-phase NMR studies indicated that the ribose sugar pucker in the self-pairing *iso*RNA duplexes[12] was C2′-*endo* (S-type). From these CD and NMR studies, it appeared that the *iso*RNA strand in the *iso*RNA : RNA duplex may be adopting the structural features of a natural DNA and thus the sugar residues would be existing in the C2′-*endo* conformation. In molecular modeling studies by Yathindra and Lalitha,[13] a critical examination of the stereochemistry of 2′–5′- and 3′–5′-linkages revealed an inverse relationship between the nucleotide geometry and involvement of either the 2′- or 3′-hydroxyl group of ribose sugar in forming the phosphodiester linkage. A 2′–5′-linkage with a C2′-*endo* sugar produces a compact nucleotide geometry

[a]*Organic Chemistry Division, CSIR-National Chemical Laboratory, Homi Bhabha Road, Pune 411008, India. E-mail: va.kumar@ncl.res.in; Fax: +91 20 2590 2629; Tel: +91 20 2590 2340*

[b]*CMC Division, CSIR-National Chemical Laboratory, Homi Bhabha Road, Pune 411008, India*

†Electronic supplementary information (ESI) available: ^{1}H & ^{13}C NMR spectra of compounds **2–7**, **10a** & **10b**; mass spectra of compounds **2–7**, **10a** & **10b**; ^{31}P NMR and mass spectra of compounds **8**, **11a** & **11b**; HPLC chromatograms of purified modified and unmodified 2′ DNA oligomers; MALDI-TOF mass spectra of 2′ DNA oligomers; MALDI-TOF mass spectra of 2′ DNA-1, 2′ DNA^{X}U^{F}-1d, 2′ DNA^{T}U^{F}-1d, 2′ DNA-U^{N}-1s and 2′ DNA-U^{S}-1s with deletion of the 2′ terminal adenosine-5′-phosphate; UV-melting plots of 2′ DNA-1 : RNA1/DNA1 and 2′ DNA-2 : RNA2/DNA2; UV-melting plots of duplexes of oligomers containing U^{S}, U^{N}, ^{X}U^{F} and ^{T}U^{F} with RNA1/RNA2; representative UV-melting plot of ss2′ DNA-U^{S}-1s, ssRNA1 and 2′ DNA-U^{S}-1s : RNA1; representative RP-HPLC chromatograms for SVPDE study with 3′DNA-1, 2′ DNA-1 and 2′ DNA-3. CCDC 900136 and 900137. For ESI and crystallographic data in CIF or other electronic format see DOI: 10.1039/c2ob26762d

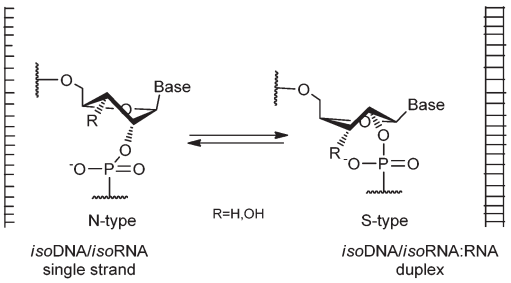

Fig. 1 Sugar conformations of 2′–5′ nucleoside in single-stranded *iso*DNA/*iso*RNA and double-stranded *iso*DNA/*iso*RNA : RNA duplex.

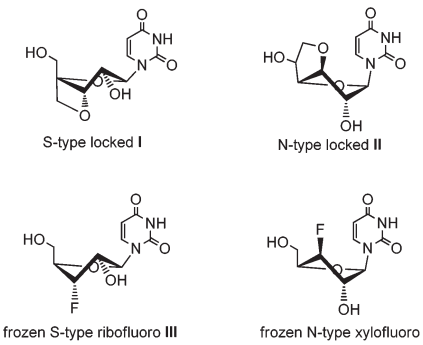

Fig. 2 S-type and N-type locked and frozen nucleosides.

whereas the 3′–5′-linkage with the same C2′-*endo* sugar gives rise to an extended nucleotide geometry. Thus, to have a compact A-type overall structure of *iso*RNA : RNA duplex, the S-type or C2′-*endo* sugar pucker in the repeating nucleotides is stereochemically favoured in the *iso*RNA strand of the duplex. Similar structural requirements were reported for 2′–5′-linked *iso*DNA : RNA duplexes by both Breslow and Sheppard,[14] and Switzer *et al*.[15] CD spectroscopy[15a] and modelling studies[16] predicted that the *iso*DNA strand in *iso*DNA : RNA duplexes would predominantly have S-type sugar conformations. On the contrary, an extended structure with N-type sugar conformations was reported when NMR studies were carried out using single stranded *iso*RNA[17a] and 2′–5′-d(G_4C_4).[17b] Also, the crystal structure[18] obtained for a single strand 2′–5′-RNA showed a C3′-*endo* or N-type sugar pucker. Hence the sugar conformations (N-type) observed in an *iso*DNA/*iso*RNA single strand are not the same as that predicted for the *iso*DNA/*iso*RNA strand in an *iso*RNA/*iso*DNA : RNA duplex (S-type). In a single-stranded 2′–5′-DNA oligomer, the *gauche* and anomeric effects of the 2′-hydroxyl group would dominate the preference for 3′-*endo* (N-type) sugar conformation in the absence of a 3′-hydroxyl group. Therefore in the *iso*DNA : RNA duplex it was assumed that the RNA strand would impose its structure[19] on the *iso*DNA strand causing the individual nucleosides in the *iso*DNA to adopt C2′-*endo* conformations so as to form a stable duplex with RNA, leading to a conformationally and topologically constrained *iso*DNA in the *iso*DNA : RNA duplex (Fig. 1).[16] In view of the above discussion, we planned to study the duplex stability of *iso*DNA : RNA duplexes by applying conformational locks that would render the nucleosides to adopt either the S-type (Fig. 2, **I** and **III**) or N-type (Fig. 2, **II** and **IV**) sugar conformations. This work was inspired by the successes met especially with LNA and HNA and 2′-ribo/arabino-fluoro-substituted DNA where highly stable DNA : RNA duplexes were formed by applying appropriate conformational constraints with entropic advantages. We reported earlier[20] our preliminary results summarising the effects of incorporation of these monomer units (Fig. 2, **I–IV**) with constrained or frozen S-type/N-type sugar conformations in the *iso*DNA strand of *iso*DNA : RNA duplexes. In this paper, we further give the detailed synthesis and characterization of the constrained and frozen monomer building blocks, the effect of the constrained unit in the sequence context, site of modifications, effect of the neighbouring nucleoside using UV analysis and also the stability of the 2′–5′ linked oligomers to exonuclease degradation by SVPDE in comparison with the unmodified DNA sequences. In addition, conformational analysis of modified nucleosides is presented based on X-ray crystallographic analysis in our laboratory for 3′-deoxy-3′-ribofluorouridine, 3′-deoxy-3′-xylofluorouridine, 3′-*O*,4′-C-methylene ribonucleoside[21d] in conjunction with $^3J_{HH}$ couplings and two-dimensional NOE experiments in solution.

Results and discussion

Synthesis of monomers

The synthesis of constrained nucleoside units (Fig. 2, **II–IV**) and their protected phosphoramidite building blocks amenable for 2′–5′ linked oligonucleotide synthesis was accomplished starting from D-glucose. The S-type locked nucleoside (Fig. 2, **I**) phosphoramidite was synthesized according to literature procedure[21] using uridine as starting material. The synthesis of N-type (Fig. 2, **II**) building block is outlined in Scheme 1. Compound **1** was synthesized from the glucose diacetonide by following the earlier reported multistep synthesis procedure.[22] The free hydroxyl group in **1** (Scheme 1) was protected as its Alloc derivative to give compound **2** in 99% yield (purity >90% by NMR). The acetonide group in **2** was removed, and the compound was converted to the diacetate **3** in 75% yield by treatment with AcOH and Ac_2O in the presence of a catalytic amount of H_2SO_4. The reaction of **3** with bis(trimethylsilyl)uracil (U·2TMS) under Vorbrüggen's conditions afforded only the β-anomer of uridine derivative **4** (93%). The Alloc protecting group in **4** could be selectively cleaved in presence of the 3′-acetate using Pd(0) to get **5** (70%). The free secondary hydroxyl group in **5** was protected as its 4,4′-dimethoxytrityl (DMT) group using excess of DMT chloride and a catalytic amount of DMAP in dry pyridine to get **6** (85%). Compound **6** was then subjected to ammonolysis to give free 2′-hydroxy compound **7** (93%). Phosphitylation at the 2′-hydroxy group with *N*,*N*-diisopropylamino-2-cyanoethylphosphino-chloridite afforded the desired phosphoramidite building block **8** (60%) as N-type locked monomer. All the compounds were purified by column chromatography. All the

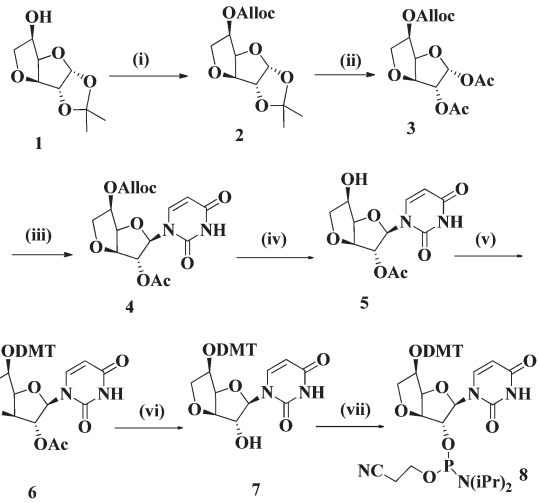

Scheme 1 Synthesis of N-type locked monomer. Reagents and conditions: (i) Dry CH_2Cl_2–dry pyridine, Alloc-Cl, 0 °C 1 h, 99%. (ii) AcOH–Ac_2O–H_2SO_4, 10 : 1.0 : 0.1, RT, 12 h, 75%. (iii) Uracil, CH_3CN, BSA, 70 °C, TMS-OTf, 0 °C, reflux, 3 h, 93%. (iv) CH_2Cl_2, PPh_3, piperidine, $Pd(dba)_2$, RT, 10 min, 70%. (v) DMTCl, dry pyridine, DMAP, 24 h, 85%. (vi) MeOH–aq.NH_3, RT, 1 h, 93%. (vii) dry CH_2Cl_2, $EtN(iPr)_2$, *N*,*N*-diisopropylamino-2-cyanoethylphosphino-chloridite, RT, 3 h, 60%.

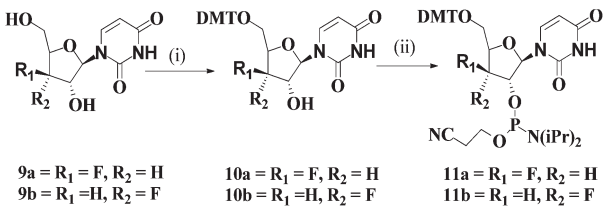

Scheme 2 Synthesis of frozen S-type and N-type fluoro monomers. Reagents and conditions: (i) DMTCl, DMAP, dry pyridine, RT, 62%. (ii) Dry CH_2Cl_2, $EtN(iPr)_2$, *N*,*N*-diisopropylamino-2-cyanoethylphosphino-chloridite, RT (**11a**, 58%; **11b**, 43%).

new compounds were appropriately characterised using ^1H, ^{13}C & ^{31}P NMR and high resolution mass spectrometric analysis. The synthesis of 3′-deoxy-3′-xylofluoro- and 3′-deoxy-3′-ribofluoro-phosphoramidite building blocks is outlined in Scheme 2. The 3′-deoxy-3′-xylofluorouridine **9a** and 3′-deoxy-3′-ribofluorouridine **9b** were synthesized from D-glucose[23] and D-xylose[24] respectively following reported procedures. Compounds **9a** and **9b** were crystallized from CH_2Cl_2–CH_3OH and analysed by X-ray crystallography. The free primary hydroxyl group in **9a**/**b** was protected with DMT group using excess of DMT chloride and a catalytic amount of DMAP in dry pyridine to give **10a**/**b** respectively with 62% yield. Phosphitylation of the 2′-hydroxy group in **10a**/**b** with *N*,*N*-diisopropylamino-2-cyanoethylphosphino-chloridite afforded the desired phosphoramidite building blocks **11a** (58%) and **11b** (43%). All compounds were purified by column chromatography. All the new compounds were appropriately characterised using ^1H, ^{13}C & ^{31}P NMR and high resolution mass spectrometric analysis.

Table 1 Conformational analysis of the nucleosides using H1′–H2′ coupling constants from ^1H NMR spectra

Nucleoside derivative	H1′–H2′ coupling *J* in Hz	%S	Reference
3′-Deoxyuridine	1.2	3	21
S-Locked uridine (U^S, **I**)	7.5	94	21
N-Locked uridine (U^N, **II**)	3.5	36	21*c*
3′-Deoxy-3′-ribofluoro-uridine ($^rU^F$, **III**)	7.7	97	24
3′-Deoxy-3′-xylofluoro-uridine ($^XU^F$, **IV**)	1.0	0.3	23

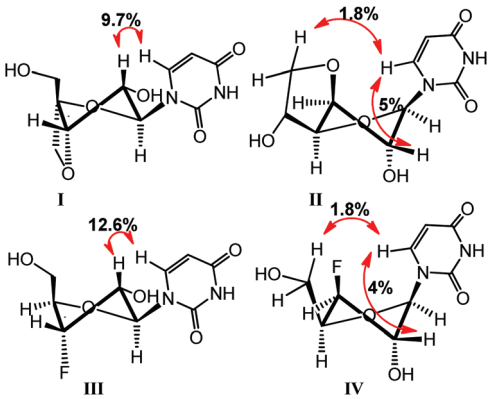

Fig. 3 Percent NOE cross peak and possible conformers for all four monomers.

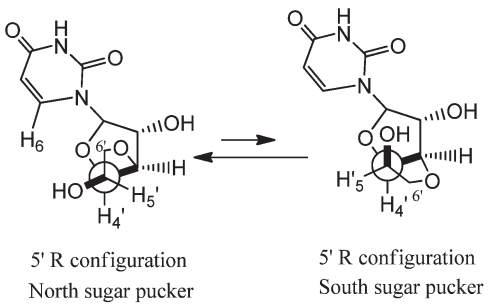

Fig. 4 Two possible conformers for N-type locked monomer due to flexible 5-membered locked ring in **II**.

Conformational analysis of nucleoside analogues

We compared the sugar conformations of 3′-deoxyuridine, the S-type/N-type locked monomer units (**I** and **II**) and also those of the 3′-ribofluoro/xylofluoro nucleoside analogues (**III**, **IV**) (Table 1, Fig. 3–5). The NOE cross peaks between H2′–H6 protons in compounds **I–IV** suggest the *anti* conformation of uracil base. The *anti* conformations of the nucleobases were also supported by χ angle obtained from the X-ray crystal structure data of **III** and **IV**.

The homonuclear $^3J_{H1'-H2'}$ coupling constants are very sensitive to the dihedral angle and therefore directly reflect the sugar pucker in five-membered ribonucleosides. %S conformation for each chosen unit was calculated from the H1′–H2′ NMR coupling constants as earlier reported.[21] A smaller

J value of 0–3 Hz is typical of N-type sugar whereas the *J* value between 6–9 Hz is indicative of S-type sugar pucker.[16] Thus, the 3′-deoxyuridine was shown to be in 97% N-type,[21] *i.e.* C3′-*endo* sugar pucker, which is consistent with the O4′–C1′–C2′–O2′ *gauche* effect as well as the anomeric effect which brings the nucleobase in pseudoaxial orientation.[19] The 3′-*O*-4′-C-methylene-linked uridine (U^S, **I**, Fig. 3 and 5) and the xylo-3′-*O*-5′-C-methylene- linked uridine (U^N, **II**, Fig. 3 and 4) would lock the monomer in S-type and N-type conformations, respectively. The crystal structural data reported earlier[21d] for thyminyl monomer of compound **I** clearly shows the structure locked in S-type sugar with a pseudorotation phase angle (*P*) of 136.2°, maximum out-of-plane pucker (ν_m) of 32.3° and the O5′–C5′–C4′–C3′dihedral angle γ in +sc range (Table 2). Our two-dimensional NOE NMR experiments revealed a strong NOE cross peak (**I**, 9.7%, Fig. 3) for the H2′ and nucleobase H6, thus confirming the 2′-*endo* sugar pucker for compound **I**, in solution also.[25] The limiting values for $J_{4'5'}$ and $J_{4'5''}$ in the staggered O5′–C5′–C4–C3′ rotamers were calculated to be as follows: Rotamer γ+ (+sc) $J_{4'5'}$ = 2.4 Hz, $J_{4'5''}$ = 1.3 Hz, Rotamer γ^t (t) $J_{4'5'}$ = 2.6 Hz, $J_{4'5''}$ = 10.5 Hz and Rotamer γ- (−sc) $J_{4'5'}$ = 10.6 Hz, $J_{4'5''}$ = 3.8 Hz.[26] In the absence of the H4′ proton in **I**, it is not possible to comment on the solution rotameric population indicated by γ but the crystal data indicated that this falls in +sc range when the base was thymine (Table 2).

In compound **II**, the flexible 5-membered ring allowed ~36% S-type character to the sugar ring, (conformational analysis based on the $^3J_{H1'-H2'}$). Two forms of the sugar conformations for **II** could be possible, in which the C5′-carbon is fixed in *R* configuration as depicted in Fig. 4. The O4′–C4′–C3′–O3′ *gauche* effect operative in N-type xylo-sugar would stabilize the N-type sugar ring conformation shifting the equilibrium to N-type. An additional proof for the sugar conformation in **II** being predominantly N-type, comes from a relatively less strong NOE cross peak (5%) between H2′ and H6.[25] An additional positive NOE cross peak (1.8%) between H6 and H6′ is observed which would indeed not be observed if S-type conformation was predominant in **II** (Fig. 3 and 4). The preferred O5′–C5′–C4–C3′ geometry would be then expected to be (γ^t) due to the fixed *R* configuration at C5′ in the preferred N-type conformer of **II**. The observed $^3J_{H4'-H5'}$ coupling (J = 4.1 Hz, ESI,† page S-3) would not be able to differentiate between the two possible structures for compound **II**, in the absence of H4′–H5″ proton for which expected *J* would be ≈10.5 Hz in North conformation, and ≈4.5 Hz for South conformation.

The monomeric conformations of 3′-deoxy-3′-ribofluorouridine ($^rU^F$, **III**), and 3′-deoxy-3′-xylofluorouridine ($^XU^F$, **IV**) were found to be almost frozen in S- and N-type conformations respectively, based on the vicinal coupling $^3J_{H1'-H2'}$. The conformational preferences are consistent with the strong O4′–C4′–C3′–F3′ *gauche* effect of fluoro-substituted nucleoside analogues over the anomeric effect of C-1′ substitution. The proof for the solution structure further comes from the observed strong NOE cross peaks as shown in Fig. 3. The NOE cross peak between the *beta* oriented H2′ and nucleobase H6 is 12.6% in **III** (the S-type sugar), whereas in compound **IV** where the N-type geometry is preferred, the observed NOE (4%) is relatively weaker (due to increased distance between the two interacting protons).[25] Further, the preferred O5′–C5′–C4–C3′ geometry in solution would be +sc for the ribofluoro derivative and is in equilibrium with −sc and t for the xylofluoro derivatives based on the $^3J_{H4'-H5'}$ and $^3J_{H4'-H5''}$[26] (ESI,† page S-3).

The conformational features based on coupling constants and NOE measurements are confirmed by X-ray crystallographic data for compounds **IV**,[23] reported earlier. We collected this data for compound **III** for the first time in the present study.‡ We also collected crystal structure data for compound **IV** for comparison. The results from these studies are depicted in Fig. 6 in the form of an ORTEP picture for compound **III**. Three crystal forms were observed and Form I is shown in Fig. 6. The superimposition of the three forms for the **III** is shown in ESI† (page S 48). The 3′-ribo-configured fluorosugar in **III** was found to be C2′-*endo*, S-type, as against the C3′-*endo*, N-type sugar conformation that was found for

‡X-ray intensity data measurements of compound **III** and **IV** were carried out on a Bruker SMART APEX II CCD diffractometer with graphite-monochromatized (MoK_α = 0.71073Å) radiation at 100(2) K. The X-ray generator was operated at 50 kV and 30 mA. A preliminary set of cell constants and an orientation matrix were calculated from 694 (for **III**) harvested from three sets of 90 frames for URF and 36 frames for UXF. Data were collected with ω scan width of 0.5° at different settings of φ and 2θ with a frame time of 10 and 5 s respectively keeping the sample-to-detector distance fixed at 5.00 cm. The X-ray data collection was monitored by APEX2 program (Bruker 2006, *APEX2*, *SAINT* and *SADABS*. Bruker AXS Inc., Madison, Wisconsin, USA.).

Crystal data of **III**. $C_9H_{11}FN_2O_5$, M = 246.20, colorless plate, 0.59 × 0.17 × 0.10 mm^3, monoclinic, space group $P2_1$, a = 15.4056(4), b = 6.8529(2), c = 15.8005(4) Å, β = 116.0190(10)°, V = 1499.04(7) Å^3, Z = 6, T = 100(2) K, $2\theta_{max}$ = 56.00°, D_{calc} (g cm^{-3}) = 1.636, $F(000)$ = 768, μ (mm^{-1}) = 0.146, 24 993 reflections collected, 7180 unique reflections (R_{int} = 0.0295), 6731 observed ($I > 2\sigma(I)$) reflections, multi-scan absorption correction, T_{min} = 0.919, T_{max} = 0.986, 484 refined parameters, S = 1.067, R_1 = 0.0342, wR_2 = 0.0861 (all data R = 0.0376, wR_2 = 0.0882), maximum and minimum residual electron densities; $\Delta\rho_{max}$ = 0.30, $\Delta\rho_{min}$ = −0.22 (e Å^{-3}). The asymmetric unit contains three symmetry independent molecules. Structure overlay of all the three symmetry independent molecules shows major conformational difference at the orientation of uracil moiety. The OH group at C2′ and CH_2OH group at C4′ also showed noticeable difference.

Crystal data of **IV** $C_9H_{11}FN_2O_5$, M = 246.20, colorless plate, 0.58 × 0.30 × 0.22 mm^3, monoclinic, space group $P2_1$, a = 6.3007(3), b = 7.3372(3), c = 10.8989(4) Å, β = 92.277(2)°, V = 503.45(4) Å^3, Z = 2, T = 100(2) K, $2\theta_{max}$ = 56.00°, D_{calc} (g cm^{-3}) = 1.624, $F(000)$ = 256, μ (mm^{-1}) = 0.144, 10 593 reflections collected, 2440 unique reflections (R_{int} = 0.0175), 2398 observed ($I > 2\sigma(I)$) reflections, multi-scan absorption correction, T_{min} = 0.921, T_{max} = 0.969, 162 refined parameters, S = 1.054, R_1 = 0.0239, wR_2 = 0.0643 (all data R = 0.0242, wR_2 = 0.0645), maximum and minimum residual electron densities; $\Delta\rho_{max}$ = 0.27, $\Delta\rho_{min}$ = −0.17 (e Å^{-3}). All the data were corrected for Lorentzian, polarization and absorption effects using SAINT and SADABS programs (Bruker, 2006). SHELX-97 was used for structure solution and full matrix least-squares refinement on F^2 (G. M. Sheldrick, *Acta Crystallogr.*, 2008, **A64**, 112).

Hydroxyl H-atoms compounds **III** were located in difference Fourier map and refined isotropically. Other H-atoms in both structures were placed in geometrically idealized position and constrained to ride on their parent atoms.

NOESY experiments were performed on a Bruker AV 400 MHz NMR spectrometer, and data was analyzed using the Bruker TOPSpin 1.3 software. The spectra were collected at 25 °C with 1 s mixing time. The total acquisition time of each two-dimensional experiment was 2–4 hours and 8–16 scans were taken. Percent nOe were calculated from the sub spectra of the row passing through nosey, and the diagonal peak area has been assigned as 100.

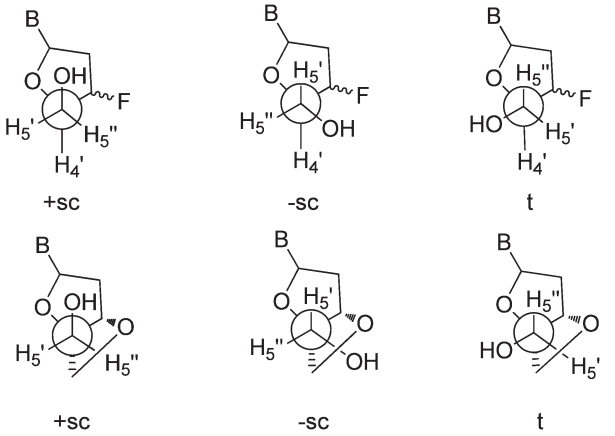

Fig. 5 Preferred conformers for **I**, **III**, and **IV**.

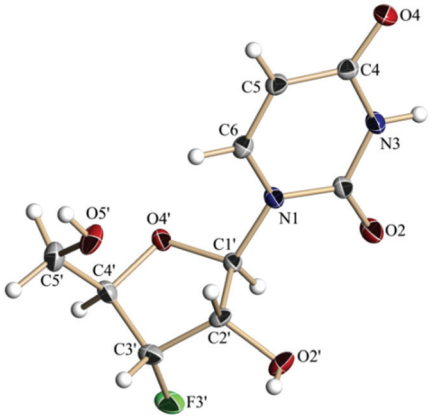

Fig. 6 ORTEP Drawing for compound **III**.

the 3′-xylo-configured fluorosugar in compound **IV** (ESI,† page S48), also reported earlier. Using the information available from the X-ray studies, it can be deduced that the sugar pucker pseudorotation phase angle (*P*) for form I crystals of compound **III** is 171.2° and the maximum out of the plane pucker (ν_{max}) is 38.6°, that is characteristic of C2′-*endo*, S-type sugar pucker (Table 2). The geometric parameters for compound **IV** were found to be concurring with C3′-*endo*, N-type sugar pucker (pseudorotation phase angle (*P*) for crystals of compound **IV** is 0.88° and the maximum out of the plane pucker (ν_{max}) is 37.6°, that is characteristic of C3′-*endo*, N-type sugar pucker). The preferred O5′–C5′–C4–C3′ geometry is consistent (γ +sc range) with the NMR solution studies for compound **III**, whereas in the case of compound **IV**, the O5′–C5′–C4–C3′ geometry was found to be γ^t range in the crystal structure (Table 2).

Synthesis of oligomers and UV-melting studies

The two sequences of the current study are of biological relevance: DNA-1 is used for miRNA down-regulation[27] and DNA-2 is used in the splice-correction assay developed by Kole *et al.*,[28] The oligomers were synthesized using an automated Bioautomation DNA synthesizer and commercially available 5′-*O*-DMT-3′-deoxy-2′-phosphoramidites. The modified units were incorporated at pre-determined positions using an extended coupling time to yield the modified oligomers efficiently. The site of the modified units in the sequences was chosen so that these were either separated by 4–5 nucleosides or were consecutive. Also, the 3′-end neighbour could be a purine or pyrimidine. The synthesized oligomers (Table 3, entry no. 1–18) were purified by HPLC subsequent to ammonia treatment and characterized by MALDI-TOF–TOF mass spectrometric analysis. Their purity was also re-checked by analytical HPLC and found to be >95% prior to their use in experiments. The thermal stability of the *iso*DNA duplexes with complementary DNA/RNA was evaluated by UV-melting studies. The melting temperatures, T_ms, of the complexes containing the S-type and N-type locked (U^S & U^N) and frozen ($^rU^F$ & $^XU^F$) units were determined and compared with the unmodified duplexes formed using 2′ DNA-1 (Table 3, entry 1) and 2′-DNA-2 (Table 3, entry 12). The results obtained for the *iso*DNA : RNA complexes are summarized in Table 3. Similar to the *iso*RNA sequences reported by Damha *et al.*,[9] the *iso*DNA sequences studied here (Table 3, entries 1–18) were also found to bind only to complementary RNA and not to

Table 2 Geometrical parameters obtained from X-ray crystal structure for compounds **I**, **III** and **IV**

	3′-Deoxy-3′-ribofluoro-uridine ($^rU^F$, III)				
	Mol A	Mol B	Mol C	3′-Deoxy-3′-xylofluoro-uridine ($^XU^F$, IV)	S-Locked thymine (T^S)
Torsion angles (°)					
ν_0 = [C4′–O4′–C1′–C2′]	−18.12(18)	−7.84(17)	−35.54(16)	11.58(10)	−29.6
ν_1 = [O4′–C1′–C2′–C3′]	34.95(17)	26.27(16)	35.24(17)	−30.98(11)	32.42
ν_2 = [C1′–C2′–C3′–C4′]	−38.14 (16)	−34.03(16)	−21.94(18)	37.52(10)	−23.5
ν_3 = [C2′–C3′–C4′–O4′]	28.46(17)	30.32(17)	2.00(18)	−31.59(10)	7.12
ν_4 = [C3′–C4′–O4′–C1′]	−6.57(18)	−14.32(17)	21.35(17)	12.76(10)	14.22
χ = [O4′–C1′–N1–C2]	−128.73(16)	−149.70(14)	−178.67(14)	−164.34(8)	−107.95
γ = [O5′–C5′–C4′–C3′]	50.5(2)	42.0(2)	49.9(2)	−172.13(9)	74.0
Pseudorotation parameters (°)					
Phase angle (*P*)	171.2	185.7	126.8	0.88	136.31
Puckering amplitude(V_m)	38.60	34.16	36.62	37.59	32.50

Table 3 Oligonucleotide sequences, characterization using MALDI-TOF mass analysis and comparative UV-T_m values

Entry no.	Sequence code	Sequence (5′ → 2′)	$Mass_{calcd.}/Mass_{obsd.}$	T_m °C RNA	ΔT_m (°C)
1	2′ DNA-1	CACCATTGTCACACTCCA	5364/5362	50.5	0.0
2	2′ DNA-U^N-1s	CACCATTGTCACACU^NCCA	5377/5376	49.4	−1.1
3	2′ DNA-U^N-1d	CACCATTGU^NCACACU^NCCA	5391/5391	42.8	−7.7
4	2′ DNA-U^S-1s	CACCATTGTCACACU^SCCA	5377/5380	51.0	+0.5
5	2′ DNA-U^S-1d	CACCATTGU^SCACACU^SCCA	5391/5393	52.8	+2.3
6	2′ DNA-U^S-1d2	CACCA$U^S$$U^S$GTCACACTCCA	5391/5390	48.5	−2.0
7	2′ DNA-$^XU^F$1s	CACCATTGTCACAC$^XU^F$CCA	5368/5365	45.7	−4.8
8	2′ DNA-$^XU^F$-1d	CACCATTG$^XU^F$CACAC$^XU^F$CCA	5372/5374	44.5	−6.0
9	2′ DNA-$^rU^F$-1s	CACCATTGTCACAC$^rU^F$CCA	5368/5366	50.5	0.0
10	2′ DNA-$^rU^F$-1d	CACCATTG$^rU^F$CACAC$^rU^F$CCA	5372/5372	51.7	+1.2
11	2′ DNA-$^rU^F$-1d2	CACCA$^rU^F$$^rU^F$GTCACACTCCA	5372/5373	49.2	−1.3
12	2′ DNA-2	CCTCTTACCTCAGTTACA	5369/5368	46.0	0.0
13	2′ DNA-U^N-2s	CCTCTTACCTCAGTU^{N}ACA	5383/5386	46.4	+0.4
14	2′ DNA-U^N-2d	CCTCTTACCU^{N}CAGTU^{N}ACA	5397/5396	41.9	−4.1
15	2′ DNA-U^S-2s	CCTCTTACCTCAGTU^{S}ACA	5383/5385	47.0	+1.0
16	2′ DNA-U^S-2d	CCTCTTACCU^{S}CAGTU^{S}ACA	5397/5395	46.7	+0.7
17	2′ DNA-$^rU^F$-2s	CCTCTTACCTCAGT$^rU^F$ACA	5373/5376	48.3	+2.3
18	2′ DNA-$^rU^F$-2d	CCTCTTACC$^rU^F$CAGT$^rU^F$ACA	5377/5379	49.4	+3.4

Melting temperatures (T_ms) were obtained from the maxima of the first derivatives of the melting curves ($A_{260\ nm}$ *versus* temperature), measured in buffer containing 10 mM sodium phosphate, 150 mM sodium chloride, pH 7.4, using 1 μM concentration of each of the two complementary strands. Each experiment was repeated at least thrice and the values are accurate to ±0.5 °C. Complementary RNA sequences for DNA-1 and DNA-2 are RNA-1 and RNA-2 respectively. RNA1 = 5′-UGGAGUGUGACAAUGGUG-3′. RNA2 = 5′-UGUAACUGAGGUAAGAGG-3′. T_m of 2′ DNA-1 : cDNA-1 = 59.0 °C and 2′ DNA-2 : cDNA-2 = 54.0 °C. $\Delta T_m = T_m - T_{m(control)}$.

complementary DNA (ESI,† page S-41–46). Sharp, well-defined sigmoid-shaped melting curves were observed for the complexes with complementary RNA with a 10–20% hyperchromicity at 260 nm, while, for the complexes with complementary DNA, there was no sigmoid transition, indicating no complexation in the latter case. As reported in our earlier communication,[20] for complexes containing modified/unmodified 2′ DNA-1, the S-type locked units were found to favour stable complex formation with the complementary RNA, while the N-type locked units caused a destabilization of the resulting complexes with complementary RNA. This stabilizing/destabilizing effect was found to increase with an increase in the number of modified units. Thus, the inclusion of two modified units (U^S or U^N) caused a larger stabilization/destabilization of the resulting complexes (ΔT_m = +2.3 & −7.7 °C respectively; Table 3, entries 5 & 3 respectively) compared to the oligomers containing only a single modified unit (ΔT_m = +0.5 & −1.1 °C respectively; Table 3, entries 4 & 2 respectively). The stabilization caused by the S-type locked monomer (U^S) and the destabilization caused by the N-type locked monomer (U^N) was in accordance with the prediction of S-type conformation for the *iso*DNA strand in an *iso*DNA : RNA duplex.[16] However, the orientation of the nucleobase in the U^S unit is pseudoequatorial, which effects weaker stacking and hydrogen-bonding interactions[18] in comparison to the instance when the nucleobase is pseudoaxial (as in the U^N unit and LNA). This could be the reason why the stability imparted by the U^S was not as large as that by LNA ($\Delta T_m \sim$ +4 °C/modification)[6] in 3′-5′-LNA : RNA duplexes. A similar effect was observed for the S- and N-type frozen units ($^rU^F$ & $^XU^F$ respectively). In this case too, the S-type frozen units ($^rU^F$) were found to effect a much more modest stabilization in comparison to the destabilizating effect caused by the N-type frozen units ($^XU^F$). Thus, the complexes containing $^XU^F$ units were destabilized to a much greater extent (ΔT_m = −4.8 & −6.0 °C respectively, for complexes containing one and two modified units respectively; Table 3, entries 7 & 8 respectively) in comparison to the stabilization observed for complexes containing $^rU^F$ units (ΔT_m = 0.0 & +1.2 °C respectively, for complexes containing one and two modified units; Table 3, entries 9 & 10 respectively). This could be due to the inability of the S-type frozen conformation to further strengthen the stacking and hydrogen-bonding interactions when the nucleobase is oriented pseudoequatorially. The O4′–C4′–C3′–F3′ *gauche* effect is probably responsible for the resistance to the N- to S-type conformational change that must take place in adopting the duplex state, considering comparable steric interactions between the fluorine and hydrogen atoms.[23,24,29] This dominating O4′–C4′–C3′–F3′ *gauche* effect is again responsible for the preferred sugar pucker in the $^rU^F$/$^XU^F$derivative. To study the additive stabilization effect of the conformational constraint, we modified consecutive sites in DNA-1 as in 2′ DNA-U^S-1d2 and 2′ DNA-$^rU^F$-1d2 (entries 6, 11, Table 3). In either case, the consecutive modified sites were not able to cause additive stabilization. In fact, the duplexes formed were marginally destabilized ($\Delta T_m \approx$ −1.5 °C). This result is also in contrast to the 3′-5′ LNA : RNA duplexes where consecutive modified units show much better stabilization due to increased base-stacking interactions when the nucleobases are axially oriented.[6]

To further study the effect of modifications in the sequence context and the site of modifications, we synthesized another sequence 2′ DNA-2 (entry 12, Table 3), and oligomers having one or two S-type locked (U^S), N-type locked (U^N) and

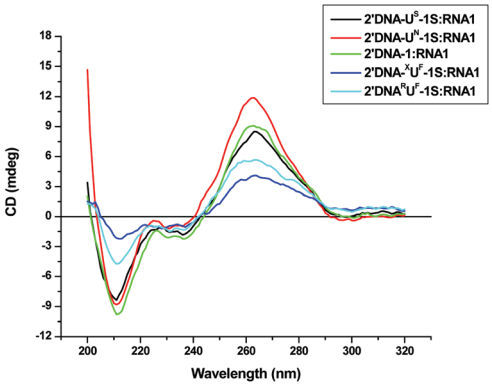

Fig. 7 Duplex CD spectra for complexes derived from **I–IV**.

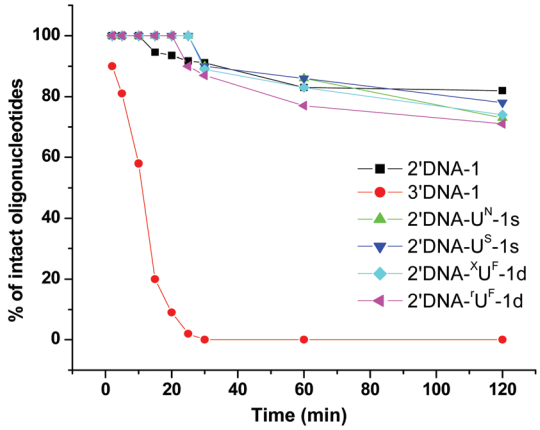

Fig. 8 Stability assay of the ONs to degradation by SVPDE. #In the case of 2′ DNA oligomers, the 2′-end adenine nucleoside-5′-phosphate is cleaved (ESI,† page S-39–40).

ribofluoro ($^{r}U^{F}$) monomeric units (2′ DNA-U^{N}-2s, 2′ DNA-U^{N}-2d, 2′ DNA-U^{S}-2s, 2′ DNA-U^{S}-2d, 2′ DNA-$^{r}U^{F}$-2s, 2′ DNA-$^{r}U^{F}$-2d (Table 3, entries 13–18 respectively) and compared the stability of the duplexes in terms of T_m-studies with the unmodified control duplex (2′ DNA-2 : RNA-2). The modified units were spaced by four unmodified units. The results were qualitatively similar to those observed for DNA-1. The N-type locked monomer again caused destabilization of the resulting duplex whereas the S-type locked/frozen units stabilized the duplex with complementary RNA. In fact, the 3′-deoxy-3′-ribofluorouridine-derived sequences stabilized the duplex much better ($\Delta T_m \sim +2$ °C/modification, entries 17, 18, Table 3). In the sequence context, the difference is that one of the modified units is flanked by a purine instead of pyrimidine at the 2′-end. The result presented in this paper thus confirms that in *iso*DNA : RNA duplexes, the DNA strand would prefer to assume S-type geometry that is complemented by S-type locked and S-type frozen nucleoside units and the stability would be improved further, depending on the flanking base sequence.

As an additional support for duplex formation in all the modifications used in the present studies, CD spectroscopic studies of complexes of modified oligomers with RNA1 (entries 2, 4, 7 and 9) were also carried out. In all these cases, it was observed that the duplex CD spectra were similar for all the complexes studied (Fig. 7) and resemble A-type DNA : RNA duplex CD spectra.[30] The additive CD spectrum of the two strands (RNA1 + 2′ DNA-U^{S}-1s) was different from that for the duplex (RNA: 2′ DNA-U^{S}-1s). The overall adopted structures due to the incorporation of modified units (**I–IV**) were not found to alter the overall structural features of the complexes formed, although thermal stability was affected.

Stability of oligonucleotide to SVPDE

We examined the stability of unmodified and modified 2′-5′-linked oligonucleotides towards 3′-exonuclease [snake venom phosphodiesterase (SVPDE)] degradation and compared them with natural DNA. After incubation of each ON solution at 37 °C in the presence of SVPDE, the percentage of intact ONs was analyzed at several time-points by RP-HPLC (Fig. 8). The natural ssDNA was completely digested within 30 min. The unmodified as well as modified 2′–5′ linked 3′-deoxy-oligonucleotides were found to be considerably stable under these conditions, although the 3′-deoxy-riboadenosine-5′phosphate at the 2′-end of the oligomers was cleaved under these conditions. SVPDE is known to cleave the tetrameric 2′–5′-adenine sequences[31] and in this particular study, the sequences used happened to contain an adenine nucleoside at the 2′-end. The HPLC peak arising after this cleavage (ESI,† page S-47) was identified by MALDI-TOF mass spectrometry (ESI,† page S-39–40) as the oligomer in which one adenosine-5′-phosphate unit is deleted. To confirm this finding, we further synthesized an unmodified 2′–5′ linked 3′-deoxy oligomer (ESI,† page S-47; 2′ DNA-3, 5′-GAAGGGCTTCTTCCTTAT-2′), that has a thymine nucleoside at the 2′-end. This oligomer was found to be stable towards nucleolytic cleavage. Thus, the 2′–5′ oligonucleotides were found to be resistant to digestion by the 3′-exonuclease except for the hydrolytic cleavage of the 2′-terminal adenosine-5′-phosphate.

Experimental

General

All the reagents were purchased from Sigma-Aldrich and used without further purification. SVPDE was purchased from Sigma. DMF, pyridine were dried over KOH and 4 Å molecular sieves. TLCs were run on pre-coated silica gel GF254 sheets (Merck 5554). All reactions were monitored by TLC and usual workup implies sequential washing of the organic extract with water and brine followed by drying over anhydrous sodium sulfate and evaporation under vacuum. Column chromatography was performed for purification of compounds on silica gel (60–120 mesh or 100–200 mesh, Merck). TLCs were performed using dichloromethane–methanol or petroleum ether–ethyl acetate solvent systems for most compounds. Compounds were visualized with UV light and/or by spraying with

30% perchloric acid–EtOH solution and heating. ^{1}H (200 MHz) and ^{13}C (50 MHz) NMR spectra were recorded on a Bruker ACF 200 spectrometer fitted with an Aspect 3000 computer and ^{31}P NMR spectra were recorded on a 400 MHz Bruker ACF instrument. All the chemical shifts (δ/ppm) are referred to internal TMS for ^{1}H and chloroform-d/DMSO-d_6 for ^{13}C NMR. ^{1}H NMR data are reported in the order of chemical shift, multiplicity (s, singlet; d, doublet; t, triplet; m, multiplet and/or multiple resonance), number of protons. Mass spectra were recorded on a APQSTAR spectrometer, LC-MS on a Finnigan-Matt instrument. DNA oligomers were synthesized on CPG solid support using Bioautomation Mer-Made 4 synthesizer. The RNA oligonucleotides were obtained commercially (Sigma-Aldrich). RP-HPLC was carried out on a C18 column using either a Varian system (Analytical semi-preparative system consisting of Varian Prostar 210 binary solvent delivery system and Dynamax UV-D2 variable wavelength detector and Star chromatography software) or a Waters system (Waters Delta 600 e quaternary solvent delivery system and 2998 photodiode array detector and Empower2 chromatography software). MALDI-TOF spectra were recorded on a Voyager-De-STR (Applied Biosystems) MALDI-TOF instrument or a AB Sciex TOF/TOF™ Series Explorer™ 72 085 instrument and the matrix used for analysis was THAP (2′,4′,6′-trihydroxyacetophenone). UV experiments were performed on a Varian Cary 300 UV-VIS spectrophotometer fitted with a Peltier-controlled temperature programmer. CD spectra were recorded on a Jasco J-715 Spectropolarimeter, with a ThermoHaake K20 programmable water circulator for temperature control of the sample.

5-*O*-Allyloxy-3,6-anhydro-1,2-isopropylidene-glucofuranose (2)

3,6-Anhydro-1,2-isopropylidene-5-hydroxy-glucofuranose (0.46 g, 2.28 mmol) was dissolved in dry dichloromethane (9 ml). Anhydrous pyridine (0.38 ml) was added and the reaction mixture was cooled to 0 °C in an ice-bath. Allyloxycarbonyl chloride (0.3 ml, 2.91 mmol) was added dropwise and then the reaction was stirred at room temperature for two hours, when TLC showed absence of starting compound. The reaction mixture was extracted with dichloromethane, followed by water wash and drying over sodium sulfate. Removal of solvent yielded a sticky gum of compound **2**, which was used without any further purification. Yield: 0.650 g, >90% by NMR. ^{1}H NMR ($CDCl_3$, 200 MHz): δ 1.34 (s, 3H, CH_3), 1.49 (s, 3H, CH_3), 3.78–3.86 (m, 1H, H6), 4.00–4.08 (m, 1H, H6′), 4.54–4.56 (d, 1H, J = , H5), 4.61–4.67 (m, 3H, H2, H3, H4), 4.99–5.09 (m, 2H, allyl-H), 5.25–5.43 (m, 2H, allyl-H), 5.84–6.03 (bm, 1H, allyl-H) 6.00 (d, 1H, H1, J = 3.55 Hz). ^{13}C NMR ($CDCl_3$, 50 MHz): δ 26.7, 27.3, 66.7, 68.8 76.0, 80.7, 84.8, 85.2 107.1, 112.7, 119.1, 131.1, 154.1. HRMS(ESI) calcd for $C_{13}H_{19}O_7$ (M + H^+) 287.1125, found: 287.1123.

1,2-Di-*O*-acetyl-3,6-anhydro-5-*O*-allyloxy-α,β-glucofuranose (3)

Compound **2** was desiccated (1.50 g, 0.52 mmol) and dissolved in acetic acid (16 ml). Acetic anhydride (1.6 ml) was added, after cooling the reaction flask to 10 °C, followed by dropwise and slow addition of concentrated sulfuric acid (0.16 ml). The reaction mixture was stirred overnight at room temperature. TLC indicated complete product formation. The reaction was quenched with ice and 5% aqueous $NaHCO_3$, then extracted with dichloromethane, followed by water wash and drying over sodium sulfate. After solvent removal the crude product was purified by silica gel column chromatography using petroleum ether and ethyl acetate as eluants. The compound **3** was eluted in 30% ethyl acetate in petroleum ether. Yield: 1.32 g, 76.3% ^{1}H NMR ($CDCl_3$, 200 MHz): δ 2.07 (s, 3H, CH_3), 2.09 (s, 3H, CH_3), 3.84–3.92 (m, 1H, H6), 4.05–4.11 (m, 1H, H6′), 4.64–4.67 (m, 2H, H3, H4), 4.75–4.80 (m, 1H, H2), 4.95–5.0 (m, 2H, allyl-H), 5.26–5.41 (m, 2H, allyl-H), 5.84–6.23 (m, 1H, allyl-H), 6.52 (d, 1H, H1, J = 4.2 Hz). ^{13}C NMR ($CDCl_3$, 50 MHz): δ 20.3, 20.75, 68.4, 68.5, 74.9, 80.3, 83.0, 85.2, 100.2, 118.7, 131.0, 153.8, 169.0. IR ($CHCl_3$): ν_{max} (cm^{-1}) 3024, 1749, 1650, 1428.16, 1371.84 1266.85 1114.45, 1061.37, 1024.79, 957.51, 879.82, 755.49, 667.5, 599.59. HRMS(ESI) calcd for $C_{14}H_{18}O_9Na$ (M + Na+) 353.0843, found: 353.080.

2′-*O*-Acetyl-3′,6′-anhydro-5′-*O*-allyloxy-uridine (4)

Compound **3** (1.11 g, 3.36 mmol), obtained from the previous step was dissolved in anhydrous acetonitrile (35 ml). The reaction flask was flushed with nitrogen and uracil (0.45 g, 4.03 mmol) was added. *N*,*O*-Bis(trimethylsilyl)acetamide (BSA) (0.27 ml, 1.1 mmol) was added to the reaction flask under nitrogen atmosphere. Then the reaction mixture was refluxed at 70 °C for one hour, followed by cooling in an ice bath. TMSOTf (0.23 ml, 1.27 mmol) was added slowly with a syringe and the reaction mixture was refluxed for three hours. TLC showed disappearance of starting material and appearance of a lower moving UV-positive spot which charred on acid spraying and heating. The reaction mixture was cooled to room temperature, diluted with dichloromethane, washed with $NaHCO_3$ and water, dried over sodium sulfate followed by solvent removal. The crude product was purified by silica gel column chromatography using dichloromethane and methanol as eluants. Compound **4** eluted in 2.5% methanol in dichloromethane. Yield: 1.19 g, 92.96%. ^{1}H NMR ($CDCl_3$, 200 MHz): δ 2.13 (s, 3H, CH_3), 4.09–4.12 (m, 2H, H6′, H6″), 4.54–4.57 (m, 1H, H4′), 4.62–4.66 (m, 2H, H3′, H2′), 4.93–4.98 (m, 1H, H5′), 5.15–5.41 (bm, 4H, allyl-H), 5.78–5.83 (dd, 1H, J = 10.53, 2.14 Hz, H5) 5.84–6.01 (m, 1H, allyl-H), 6.24 (d, 1H, H1′, J = 3.88 Hz), 7.62 (d, 1H, J = 8.21 Hz, H6), 8.84 (bs, 1H, NH). ^{13}C NMR ($CDCl_3$, 50 MHz): δ 20.4, 69.0, 70.9, 76.0, 79.2, 81.2, 85.5, 90.5, 103.4, 119.4, 130.8, 139.7, 150.3, 153.9, 163.1, 169.4. IR ($CHCl_3$): ν_{max} (cm^{-1}) 3391.85, 3020.46, 2924.68, 2853.76, 1751.23, 1694.89, 1458.89, 1381.57, 1265.47, 1216.15, 1090.08, 1060.10, 758.86, 668.59. HRMS(ESI) calcd for $C_{16}H_{19}O_9N_2$ (M + H^+) 383.1085, found: 383.1086.

5′-Hydroxy-2′-*O*-acetyl-3′,6′-anhydro-uridine (5)

Compound **4** (1.19 g, 3.14 mmol) obtained in the previous step, was dissolved in dichloromethane (45 ml). PPh_3 (0.54 g, 2.06 mmol) was added, followed by piperidine (2.0 ml, 0.02 mmol) and tris(dibenzylideneacetone)dipalladium [$Pd_2(dba)_3$] (0.15 g, 0.16 mmol). The reaction mixture was

stirred for 10 minutes. TLC showed absence of starting compound. Solvent was removed and the crude product was given a wash with solvent ether. Column purification done on a silica gel column yielded the pure compound **5**, which eluted in methanol (3.5%) in dichloromethane. Yield: 0.65 g, 70%. ^{1}H NMR ($CDCl_3$, 500 MHz): δ 2.13 (s, 3H, CH_3), 2.75 (d, 1H, J = 7.98 Hz, OH), 3.85–3.88 (m, 1H, H6″), 4.04–4.08 (m, 1H, H6′), 4.51–4.52 (m, 2H, H4′, H5′), 4.71–4.72 (m, 1H, H3′), 5.28–5.29 (m, 1H, H2′) 5.82 (d, 1H, H5, J = 8.19 Hz), 6.23 (d, 1H, H1′, J = 3.6 Hz), 7.59 (d, 1H, H6, J = 8.32 Hz), 8.45 (s, 1H, NH). ^{13}C NMR ($CDCl_3$, 50 MHz): δ 20.5, 72.3, 73.8, 79.8, 82.7, 85.5, 91.3, 103.8, 140.4, 150.0, 162.4, 169.5. HRMS(ESI) calcd for $C_{12}H_{15}O_7N_2$ (M + H^+) 299.0874, found: 299.0873.

5′-*O*-Dimethoxytrityl-2′-*O*-acetyl-3′,6′-anhydro-uridine (6)

The substrate 5 (0.43 g, 1.44 mmol) was co-evaporated with anhydrous pyridine twice, and then dissolved in anhydrous pyridine (10 ml). 4,4′-Dimethoxytrityl chloride (1.46 g, 4.32 mmol) was added in one lot. The reaction mixture was stirred overnight at room temperature, when TLC showed a faster moving trityl-positive spot which charred on acid spraying and heating. The reaction was quenched with methanol, extracted with dichloromethane, washed with $NaHCO_3$ and water, dried over sodium sulfate, followed by solvent removal. The crude product was purified by silica gel column chromatography using dichloromethane, methanol and pyridine (0.5%) as eluants. Compound **6** is eluted in methanol (1.5%) in dichloromethane. Yield: 0.73 g, 84.3%. ^{1}H NMR ($CDCl_3$, 200 MHz): δ 2.09 (s, 3H, CH_3), 3.22–3.44 (m, 2H, H6′, H6″), 3.80 (s, 6H, OCH_3), 4.13–4.30 (m, 3H, H4′, H3′, H2′), 5.14–5.16 (m, 1H, H5′), 5.79 (d, 1H, H5, J = 8.10 Hz), 6.05 (d, 1H, H1′, J = 3.4 Hz), 6.82–6.87 (m, 4H, DMT), 7.31–7.5 (m, 9H, DMT), 7.81 (d, 1H, H6, J = 8.17 Hz), 8.65 (s, 1H, NH). ^{13}C NMR ($CDCl_3$, 50 MHz): δ 20.6, 55.3, 70.9, 74.3, 80.5, 82.5, 84.7, 87.6, 90.5, 103.0, 113.4, 172.2, 172.9, 128.1, 130.0, 135.8, 136.0, 139.8, 144.8, 149.7, 150.3, 158.8, 163.1, 169.4. HRMS(ESI) calcd for $C_{33}H_{32}O_9N_2Na$ (M + Na^+) 623.2000, found: 623.2000.

5′-*O*-Dimethoxytrityl-2′-hydroxy-3′,6′-anhydro-uridine (7)

The substrate **6** (0.70 g, 1.16 mmol) was dissolved in AR grade methanol (50 ml). Aqueous ammonia (15 ml) was added and the pinkish slightly turbid reaction mixture was stirred for one hour at room temperature. TLC showed the absence of starting compound. The solvents were removed to get a yellowish solid. The solid was redissolved in dichloromethane and given a water wash. The organic layer was dried over sodium sulfate and concentrated to get a pale yellow solid foam. Purification was done by silica gel column chromatography using dichloromethane, methanol and pyridine (0.5%) as eluants. Compound **7** eluted in methanol (2.5%) in dichloromethane.

Yield: 0.62 g, 93.2%. ^{1}H NMR ($CDCl_3$, 200 MHz): δ 3.18–3.34 (m, 2H), 3.79 (s, 6H), 4.16–4.17 (d, 1H, J = 3.52 Hz), 4.33–4.44 (m, 2H), 5.71 (d, 1H, J = 8.1 Hz) 5.77 (s, 1H), 6.83–6.86 (m, 4H), 7.27–7.51 (m, 9H) 8.30 (d, 1H, J = 8.1 Hz), 10.16 (bs, 1H). ^{13}C NMR ($CDCl_3$, 50 MHz): 55.2, 72.2, 75.1, 80.1, 85.3, 86.7, 88.0, 96.0, 101.3, 113.3–113.4, 123.8, 127.1, 127.8, 128.1, 129.9, 135.8, 136.0, 136.0, 140.6, 144.9, 149.6, 150.8 158.8, 164.2. HRMS(ESI) calcd for $C_{31}H_{30}O_8N_2Na$ (M + Na^+) 581.1894, found: 581.1896.

5′-*O*-Dimethoxytrityl-3′-*O*,5′-*C*-methylene(uridine) xylonucleoside-2′-*O*-phosphoramidite (8)

Compound 7 (0.20 g, 0.36 mmol) was co-evaporated with dry dichloromethane, and then dissolved in dry dichloromethane (3.0 ml). Diisopropylethylamine (DIPEA) (0.19 ml, 1.07 mmol) was added, followed by chloro(2-cyanoethoxy)-*N*,*N*-diisopropylamino)-phosphine (0.16 ml, 0.72 mmol) at 0 °C. The reaction mixture was stirred under argon atmosphere at room temperature for 3 hours, when TLC indicated the absence of starting material. The reaction mass was diluted with dichloromethane, washed with $NaHCO_3$ and water, dried over sodium sulfate, followed by solvent removal. The crude product was purified by silica gel column chromatography using a 1 : 1 mixture of dichloromethane : ethyl acetate and 1% triethylamine. Yield: 0.16 g, 58.9%.^{31}P NMR ($CDCl_3$, 50 MHz): δ 150.7, 152.0. HRMS(ESI) calcd for $C_{40}H_{49}O_9N_4$(M + H^+) 759.3153 found: 759.3155, $C_{40}H_{48}O_9N_4Na$ (M + Na^+) 781.2973 found: 781.2974, and $C_{40}H_{49}O_9N_4K$ (M + K^+) 797.2712 found: 797.2712.

5′-*O*-Dimethoxytrityl-3′-deoxy-3′-fluoro-xylofuranosyluridine (10a)[23]

A mixture of compound **9a** (0.50 g, 2.03 mmol), 4,4′-dimethoxytrityl chloride (0.67 g, 2.03 mmol) and 4-dimethylaminopyridine (0.03 g, cat.) were dissolved in pyridine (5.0 ml). The reaction mixture was stirred at room temperature for 2 h. The pyridine was removed under vacuum. The residue was dissolved in ethyl acetate (100 ml), washed with saturated $NaHCO_3$ (2 × 50 ml) and saturated aqueous NaCl (2 × 30 mL). The ethyl acetate layer was dried over Na_2SO_4, filtered and evaporated to dryness. The crude was purified by silica gel (neutralized with Et_3N) column chromatography using ethyl acetate : petroleum ether (9 : 1) to offer the title compound as a white solid. Yield: 0.70 g, 62.8%. ^{1}H NMR ($CDCl_3$, 200 MHz): ^{1}H NMR ($CDCl_3$): δ: 3.53 (m, 2H), 3.80 (s, 6H), 4.40 (d, 1H), 4.51–4.73 (m, 1H), 4.86–5.10 (dd, 1H, $J_{3',F}$ = 50.7 and $J_{3',4'}$ = 3.1 Hz), 5.63 (d, 1H, J_{65} = 8.2 Hz), 6.87 (m, 4H) 5.81(s, 1H), 7.26–7.35 (m, 9H), 7.46 (d, 1H, $J_{5,6}$ = 8.2 Hz). ^{13}C NMR($CDCl_3$, 50 MHz): δ 55.1, 60.3, 78.4, 82.8, 86.5, 93.0, 96.4, 101.7, 113.1, 126.9, 127.8, 128.0, 130.0, 135.5, 139.8, 144.3, 150.9, 158.5, 164.1. HRMS(ESI) calcd for $C_{30}H_{29}O_7N_2FNa$ (M + Na^+) 571.1851 found: 571.1852.

5′-*O*-Dimethoxytrityl-3′-deoxy-3′-fluoro-ribofuranosyluridine (10b)

A mixture of 3′-deoxy-3′-fluoro-5-hydroxy-ribofuranosyluridine **9b** (0.50 g, 2.03 mmol), 4,4′-dimethoxytrityl chloride (0.67 g, 2.03 mmol) and a catalytic amount of 4-dimethylaminopyridine were dissolved in pyridine (5 ml). The reaction mixture was stirred at room temperature for 2 h. Pyridine was removed under vacuum. The residue was dissolved in ethyl acetate (100 ml), washed with saturated $NaHCO_3$ (2 × 50 ml) and

saturated aqueous NaCl (2 × 30 ml). The ethyl acetate layer was dried over Na_2SO_4, filtered and evaporated to dryness. The crude product was purified by silica gel (neutralized with Et_3N) column chromatography using EtOAc–petroleum ether (9 : 1) to get compound **10b** as white foam. Yield: 0.70 g, 62.8%. ^{1}H NMR ($CDCl_3$, 200 MHz): δ 3.39–3.54 (m, 2H). 3.78 (s, 6H), 4.36–4.45 (m, 2H), 4.94–5.23 (dd, 1H, $J_{3',F}$ = 54.3 and $J_{3',4'}$ = 2.0 Hz), 5.45 (d, 1H, $J_{6,5}$ = 8.0 Hz), 6.15 (d, 1H, $J_{1,2}$ = 6.5 Hz), 6.84 (m, 4H), 7.22–7.33 (m, 9H),7.71 (d, 1H, $J_{5,6}$ = 8.0 Hz). ^{13}C NMR ($CDCl_3$, 50 MHz):δ 55.2, 62.7, 74.8, 82.2, 87.4, 90.0, 93.6, 103.0, 113.3, 127.2, 128.0, 129.9, 134.8, 139.7, 143.8, 151.2, 158.7, 163.4. HRMS(ESI) calcd for $C_{30}H_{29}O_7N_2FNa$ (M + Na^+) 571.1851 found: 571.1848.

5′-*O*-(Dimethoxytrityl)-β-D-xylofuranosyl 3′-deoxy-3′-fluoro-uridinyl-2-*O*-phosphoramidite (11a)

Compound **10a** (0.20 g, 0.36 mmol) was co-evaporated with dry dichloromethane, and then dissolved in dry dichloromethane (3.0 ml). Diisopropylethylamine (DIPEA) (0.19 ml, 1.09 mmol) was added, followed by chloro(2-cyanoethoxy)-*N*,*N*-diisopropylamino)-phosphine (0.16 ml, 0.73 mmol) at 0 °C. The reaction mixture was stirred under argon atmosphere at room temperature for 3 hours, when TLC indicated the absence of starting material. The reaction mass was diluted with dichloromethane, washed with $NaHCO_3$ and water, dried over sodium sulfate, followed by solvent removal. The crude product was purified on a silica gel column using 1 : 1 mixture of dichloromethane : ethylacetate and 1% triethylamine. Yield: 0.16 g, 58.6%. ^{31}P NMR (50 MHz, $CDCl_3$): δ 151.4, 153.5. HRMS(ESI) calcd for $C_{39}H_{48}O_8N_4FP$ (M + H^+)749.3110 found: 749.3110 and for (M + Na^+) $C_{39}H_{47}O_8N_4FPNa$ 771.2930 found: 771.2935.

5′-*O*-(Dimethoxytrityl)-β-D-ribofuranosyl 3′-deoxy-3′-fluoro-uridinyl-2-*O*-phosphoramidite (11b)

Compound **10b** (0.20 mg) obtained from previous step was dissolved in dry DCM (3 ml) followed by the addition of *N*,*N*-diisopropylethylamine (0.18 ml, 1.09 mmol) and chloro(2-cyanoethoxy)-(*N*,*N*-diisopropylamino)-phosphine (0.15 ml, 0.72 mmol) and the reaction mixture was stirred at room temperature for 2 h. The contents were then diluted with dry DCM and washed with 5% $NaHCO_3$ solution. The organic phase was dried over anhydrous Na_2SO_4 and concentrated to get a foamy solid. The residue was dissolved in DCM and precipitated with hexane to obtain compound **11b** (0.12 g) Yield: 43%. ^{31}P NMR ($CDCl_3$): δ 151.4, 152.5. HRMS (ESI) calcd for $C_{39}H_{48}O_8N_4FP$ (M + H^+) 749.3110 found: 749.3112 and for (M + Na^+) $C_{39}H_{47}O_8N_4FPNa$ 771.2930 found: 771.2929.

Synthesis of oligonucleotides

DNA oligomers were synthesized on a CPG solid support using Bioautomation Mer-Made 4 synthesizer using standard β-cyanoethyl phosphoramidite chemistry. The 2′–5′-linked oligomers were synthesized in 2′–5′ direction using universal columns as solid support. 5-Ethyl-thiotetrazole was used as the activator. For the modified units, double coupling (300 s × 2) was performed. After synthesis, the sequences were cleaved from the support by ammonia treatment to cleave the ester functionality that joins support to the 2′-terminus of the oligomers and deprotects the exocyclic amino protecting groups used during the synthesis. RP-HPLC was carried out on a C18 column using either a Varian system (analytical semi-preparative system consisting of Varian Prostar 210 binary solvent delivery system and Dynamax UV-D2 variable wavelength detector and Star chromatography software) or a Waters system (Waters Delta 600e quaternary solvent delivery system and 2998 photodiode array detector and Empower2 chromatography software), using an increasing gradient of acetonitrile in 0.1 N triethylammonium acetate, pH 7.0, and characterized by MALDI-TOF mass spectrometry. The MALDI-TOF spectra were recorded on Voyager-De-STR (Applied Biosystems) MALDI-TOF instrument and the matrix used for analysis was THAP (2′,4′,6′-trihydroxyacetophenone). The purity was re-checked and found to be >95%.

UV-T_m measurements

The concentration was calculated on the basis of absorbance from molar extinction coefficients of the corresponding nucleobases of DNA/RNA.[32] The experiments were performed at 1 μM concentrations. The complexes were prepared in 10 mM sodium phosphate buffer, pH 7.4 containing NaCl (150 mM) and were annealed by keeping the samples at 90 °C for 2 min followed by slow cooling to room temperature and refrigeration for at least two hours prior to running the experiments. Absorbance *versus* temperature profiles were obtained by monitoring the absorbance at 260 nm from 10–85 °C at a ramp rate of 0.5 °C per minute. The data were processed using Microcal Origin 6.1 and T_m (°C) values were derived from the maxima of the first derivative plots. All values are an average of at least 3 experiments and accurate to within ±0.5 °C.

CD experiments

The samples for CD experiments were prepared as for the UV-T_m experiments. Thus, 1 μM concentration of each strand was used. The complexes were prepared in 10 mM sodium phosphate buffer, pH 7.4 containing NaCl (150 mM) and were annealed by keeping the samples at 90 °C for 2 min followed by slow cooling to room temperature and refrigeration for at least two hours prior to running the experiments. CD spectra were recorded in a 1 cm pathlength cuvette at 10 °C, as an accumulation of 3 scans, and using a resolution of 1 nm, bandwidth of 1 nm, sensitivity of 20 mdeg, response of 1 s and a scan speed of 200 nm min^{-1}.

Nuclease resistance study

Enzymatic hydrolysis of the ONs (7.5 μM) was carried out at 37 °C in buffer (100 μl) containing 100 mM Tris-HCl (pH 8.5), 15 mM $MgCl_2$, 100 mM NaCl and SVPD (2 μg, 1.2 × 10^{-4} U). Aliquots were removed at several time-points; a portion of each reaction mixture was removed and heated to 90 °C for 2 min to inactivate the nuclease. The amount of intact ONs was analyzed at several time points by RP-HPLC. The percentage of

intact ON was then plotted against the exposure time to obtain the ON degradation curve with time.

Conclusions

A detailed study comprising the 2′–5′ oligonucleotides with N-type and S-type locked/frozen nucleoside analogues was undertaken. The results indicate that in the 2′–5′ linked oligomers, the preferred geometry of nucleosides is S-type. Moreover, the S-type frozen ribofluoro uridine nucleoside was found to exhibit higher stability when flanked by a purine rather than a pyrimidine at its 2′-end. The stability of these oligomers towards SVPDE is much better compared to the natural 3′-5′ phosphodiester-linked oligomers, except for a 2′-terminal adenosine-5′-phosphate. Further work with other nucleosides is currently being carried out in our laboratory.

Acknowledgements

N. E. thanks University Grants Commission, New Delhi for senior Research Fellowship and V. A. K. thanks Wellcome Trust UK, and Council of Scientific and Industrial Research, New Delhi for research grants.

Notes and references

1 M. L. Stephenson and P. C. Zamecnik, *Proc. Natl. Acad. Sci. U. S. A.*, 1978, **75**, 285.
2 P. C. Zamecnik and M. L. Stephenson, *Proc. Natl. Acad. Sci. U. S. A.*, 1978, **75**, 280.
3 (*a*) S. Dutta, N. Bhaduri, N. Rastogi, S. G. Chandel, J. K. Vandavasi, R. S. Upadhaya and J. Chattopadhyaya, *Med. Chem. Commun.*, 2011, **2**, 206; (*b*) Y.-L. Chiu and T. M. Rana, *RNA*, 2003, **9**, 1034; (*c*) C. F. Bennet and E. E. Swayze, *Annu. Rev. Pharmacol.*, 2010, **50**, 259; (*d*) F. Lima, T. P. Prakash, H. M. Murray, G. A. Kinberger, W. Li, A. E. Chappell, C. S. Li, S. F. Murray, H. Gaus, P. P. Seth, E. E. Swayze and S. T. Crooke, *Cell*, 2012, **150**, 883.
4 (*a*) Z. Wang, *Methods Mol. Biol.*, 2011, **676**, 51; (*b*) S. Davis, B. Lollo, S. Freier and C. Esau, *Nucleic Acids Res.*, 2006, **34**, 2294.
5 (*a*) T. Imanishi and S. Obika, *Chem. Commun.*, 2002, 1653; (*b*) C. J. Leumann, *Bioorg. Med. Chem.*, 2002, **10**, 841; (*c*) P. Herdewijn, *Biochim. Biophys. Acta, Gene Struct. Expression*, 1999, **1489**, 167; (*d*) C. Mathé and C. Périgaud, *Eur. J. Org. Chem.*, 2008, 1489.
6 (*a*) A. Koshkin, S. K. Singh, P. Nielsen, V. K. Rajwanshi, R. Kumar, M. Meldgaard, C. E. Olsen and J. Wengel, *Tetrahedron*, 1998, **54**, 3607; (*b*) S. Obika, D. Nanbu, Y. Hari, J.-i. Andoh, K.-i. Morio, T. Doi and T. Imanishi, *Tetrahedron Lett.*, 1998, **39**, 5401; (*c*) D. A. Braasch and D. R. Corey, *Chem. Biol.*, 2001, **8**, 1; (*d*) B. Vester and J. Wengel, *Biochemistry*, 2004, **43**, 13233; (*e*) M. Koizumi, *Biol. Pharm. Bull.*, 2004, **27**, 453.
7 (*a*) C. Hendrix, H. Rosemeyer, I. Verheggen, F. Seela, A. Van Aerschot and P. Herdewijn, *Chem.–Eur. J.*, 1997, **3**, 110; (*b*) A. Van Aerschot, I. Verheggen, C. Hendrix and P. Herdewijn, *Angew. Chem., Int. Ed. Engl.*, 1995, **34**, 1338.
8 (*a*) R. Steffens and C. J. Leumann, *J. Am. Chem. Soc.*, 1997, **119**, 11548; (*b*) R. Steffens and C. J. Leumann, *J. Am. Chem. Soc.*, 1999, **121**, 3249; (*c*) D. Renneberg and C. J. Leumann, *J. Am. Chem. Soc.*, 2002, **124**, 5993.
9 (*a*) M. J. Damha, P. A. Giannaris, P. Marfey and L. S. Reid, *Tetrahedron Lett.*, 1991, **32**, 2573; (*b*) P. A. Giannaris and M. J. Damha, *Nucleic Acids Res.*, 1993, **21**, 4742; (*c*) M. J. Damha, B. Meng, D. Wang, C. G. Yannopoulos and G. Just, *Nucleic Acids Res.*, 1995, **23**, 3967.
10 (*a*) J. C. Wallace and M. Edmons, *Proc. Natl. Acad. Sci. U. S. A.*, 1983, **80**, 950; (*b*) I. M. Kerr and R. E. Brown, *Proc. Natl. Acad. Sci. U. S. A.*, 1978, **75**, 256.
11 M. Wasner, D. Arion, G. Borkow, A. Noronha, A. H. Uddin, M. A. Parniak and M. J. Damha, *Biochemistry*, 1998, **37**, 7478.
12 B. J. Premraj, P. K. Patel, E. R. Kandimalla, S. Agarwal, R. V. Hosur and N. Yathindra, *Biochem. Biophys. Res. Commun.*, 2001, **283**, 537.
13 V. Lalitha and N. Yathindra, *Curr. Sci.*, 1995, **68**, 68.
14 T. L. Sheppard and R. C. Breslow, *J. Am. Chem. Soc.*, 1996, **118**, 9810.
15 (*a*) T. P. Prakash, K.-E. Jung and C. Switzer, *Chem. Commun.*, 1996, 1793; (*b*) K.-E. Jung and C. Switzer, *J. Am. Chem. Soc.*, 1994, **116**, 6059.
16 B. J. Premraj, S. Raja and N. Yathindra, *Biophys. Chem.*, 2002, **95**, 253.
17 (*a*) M. Polak, M. Manoharan, G. B. Inamati and J. Plavec, *Nucleic Acids Res.*, 2003, **31**, 2066; (*b*) B. J. Premraj, S. Raja, N. S. Bhavesh, K. Shi, R. V. Hosur, M. Sundaralingam and N. Yathindra, *Eur. J. Biochem.*, 2004, **271**, 2956.
18 S. Y. Wodak, M. Y. Liu and H. W. Wyckoff, *J. Mol. Biol.*, 1977, **116**, 855.
19 W. Saenger, in *Principles of Nucleic Acid Structure*, Springer-Verlag, New York, 1984.
20 N. D. Erande, A. D. Gunjal, M. Fernandes and V. A. Kumar, *Chem. Commun.*, 2011, **47**, 4007.
21 (*a*) S. Obika, K.-i. Morio, D. Nanbu and T. Imanishi, *Chem. Commun.*, 1997, 1643–1644; (*b*) S. Obika, K.-i. Morio, D. Nanbu, Y. Hari, I. Hiromi and T. Imanishi, *Tetrahedron*, 2002, **58**, 3039; (*c*) S. Obika, K.-i. Morio, Y. Hari and T. Imanishi, *Bioorg. Med. Chem. Lett.*, 1999, **9**, 515; (*d*) S. Obika, K.-i. Morio, D. Nanbu, Y. Hari and T. Imanishi, *Chem. Commun.*, 1999, 2423–2424.
22 R. Zou and M. D. Matteucci, *Tetrahedron Lett.*, 1996, **37**, 941.
23 H. Hayakawa, F. Takai, H. Tanaka, T. Miyasaka and K. Yamaguchi, *Chem. Pharm. Bull.*, 1990, **38**, 1136.
24 I. A. Mikhailopulo, N. E. Poopeiko, T. I. Pricota, G. G. Sivets, E. I. Kvasyuk, J. Balzarini and E. De Clercq, *J. Med. Chem.*, 1991, **34**, 2195.
25 N. Zhang, S. Zhang and J. W. Szostak, *J. Am. Chem. Soc.*, 2012, **134**, 3691–3694.

26 J. Plavec, L. H. Coole, A. Sandstrom and J. Chattopadhyaya, *Tetrahedron*, 1991, **47**, 7363–7376.
27 J. Krutzfeldt, N. Rajewsky, R. Braich, K. G. Rajeev, T. Tuschl, M. Manoharan and M. Stoffel, *Nature*, 2005 **438**, 685.
28 S.-H. Kang, M.-J. Cho and R. Kole, *Biochemistry*, 1998 **37**, 6235.
29 (*a*) A. M. Kawasaki, M. D. Casper, S. M. Freier, E. A. Lesnik, M. C. Zounes, L. L. Cummins, C. Gonsalez and P. D. Cook, *J. Med. Chem.*, 1993, **36**, 831.
30 H. T. Steely Jr., D. M. Gray and R. L. Ratliff, *Nucleic Acids Res.*, 1986, **14**, 10071.
31 (*a*) K. Morita, S. Obika, T. Imanishi, Y. Kitade and M. Koizumi, *Nucleic Acids Symp. Ser.*, 2008, **52**, 637; (*b*) K. Nagaoka, S. Kito, Y. Kitamura, Y. Ueno and Y. Kitade, *Nucleic Acids Symp. Ser.*, 2009, **53**, 123; (*c*) K. Nagaoka, Y. Kitamura, Y. Ueno and Y. Kitade, *Bioorg. Med. Chem. Lett.*, 2010, **20**, 1186.
32 *Oligonucleotide Synthesis, A Practical Approach*, ed. M. J. Gait, IRL Press, Oxford, 1984.